Coevolution of phenological traits shapes plant-pollinator coexistence

François Duchenne*[1], Virginia Dominguez-García[1], Francisco P. Molina[1] & Ignasi Bartomeus[1]

[1] *Estación Biológica de Doñana (EBD-CSIC), Sevilla, Spain*

*: *corresponding author, francois.duchenne.bio@gmail.com*

Keywords: feasibility | emergent properties | morphology | structure | competition | plant | pollinator

Data availability statement:

Codes to perform simulation, to do figures and to analyse empirical networks are available here: https://github.com/f-duchenne/Evolution_pheno_vs_morpho

Empirical plant-pollinator interaction data are available here: https://doi.org/10.5281/zenodo.13270452

Competing Interest Statement:

The authors declare no competing interests.

Author contributions:

FD designed the study and performed all analyses with inputs from VDG and IB. FPM collected the data, with punctual help from IB, and identified plant and insect species. FD wrote the first draft and all authors participated to editing and writing the final version.

Abstract

Previous research has revealed how species traits determine species interactions, and how species interactions influence species coexistence. However, this hierarchical view ignores the coevolutionary feedback from species interactions to species traits and its consequences for species coexistence. Here, we developed a theoretical model to explore how the coevolution of morphological and phenological traits shape the structure and stability of mutualistic interaction networks. We found phenological traits lead to distinctive coevolutionary opportunities for species and to different emergent properties at community level than morphological traits, because they decouple mutualism and competition. Morphological coevolution led to modular and specialized interaction networks with a low structural stability, while phenological coevolution was required to achieve nested interaction networks with a higher structural stability. This suggested that phenological coevolution is key in the emergence of stable communities. Our theoretical prediction was consistent with empirical observations: across 17 empirical pollination networks we found a high proportion of phenological motifs promoting facilitation over competition, suggesting an important role of phenological coevolution in community assembly. In addition, the phenological structure of the empirical communities was a major determinant of their structural stability. Our results highlight the importance of phenological coevolution in the emergence of diverse and stable communities.

Introduction

The coevolution between organisms involved in mutualistic interactions has fascinated biologists for many centuries (1, 2), but its role in shaping community stability remains unclear (3–5). Over the last decades, the study of mutualistic communities has developed a deep understanding of the ecological determinants of their stability (6–12) but most of this work has been conducted from an ecological perspective, neglecting coevolutionary dynamics. Fragmented pieces of evidence show that species trait coevolution can affect species interaction strengths (13, 14), which affects the structure of species interaction networks (15, 16), but the consequences for community stability remains overlooked.

The few studies that have assessed the effect of coevolutionary dynamics on the stability of mutualistic communities often focus on interaction optimization through adaptive foraging (5, 17, 18), neglecting the underlying trait coevolution that determines species interactions. The type of traits that is considered and the ecological mechanisms determining species interactions from species traits, *i.e.* linkage rules, are the basic components that determine coevolutionary opportunities. Different linkage rules lead to different coevolutionary dynamics, which end up in different network structures (15, 16). In this regard, phenological and morphological matching are the most frequent linkage rules in pollination networks (19, 20), with distinctive effects on community stability (10, 21), which suggests that they would lead to different coevolutionary dynamics.

While morphological traits structure interactions in a static way, phenological traits lead to dynamic plant-pollinator interactions over time (19, 20, 22, 23). The species turnover created by phenological traits is expected to have a positive effect on community stability, because it can promote facilitation over competition, when phenologies are organized in such a way that mutualistic partners overlap in time more than competitors do (10, 21). However, because coevolution has been neglected in previous work, we do not know yet if seasonal structures that enhance community stability can emerge spontaneously from coevolutionary dynamics or not.

To investigate the effect of phenological and morphological traits on the evolutionary dynamics of mutualistic networks and their stability, we first developed a coevolutionary models, coupled with a structuralist approach to measure community stability (7). Then, we analyzed a set of 17 time-structured empirical plant-pollinator networks and tested if the signal of phenological coevolution could be detected, and we assessed how the emerging seasonal structure affects the structural stability of natural communities. Our results show how incorporating coevolution and temporal dynamics in community ecology can help to answer the longstanding question of how diverse natural communities can be stable.

Results

In our coevolutionary model each species was characterized by two gaussian traits, a morphological trait and a phenological trait, each with a mean and a variance. Species interaction strengths were defined by the overlap between their gaussian traits: the morphological match ($0 \leq \varphi \leq 1$) and temporal co-occurrence ($0 \leq \tau \leq 1$). Between guilds, species interacted mutualistically proportionally to the product of their morphological match and temporal-co-occurrence ($\varphi\tau$). Within guilds, species competed proportionally to their amount of simultaneous shared mutualistic interactions (*cf.* Methods). We let species co-evolve for 2000 time steps and for each simulation, we tracked the trait values, the emerging interaction network structure, and the structural stability of the full community over time. To assess the distinctive effects of phenological *versus* morphological coevolution on community-level outputs we performed three sets of simulations: with phenological and morphological traits (mixed coevolution), with morphological trait only (morphological coevolution) and with phenological trait only (phenological coevolution).

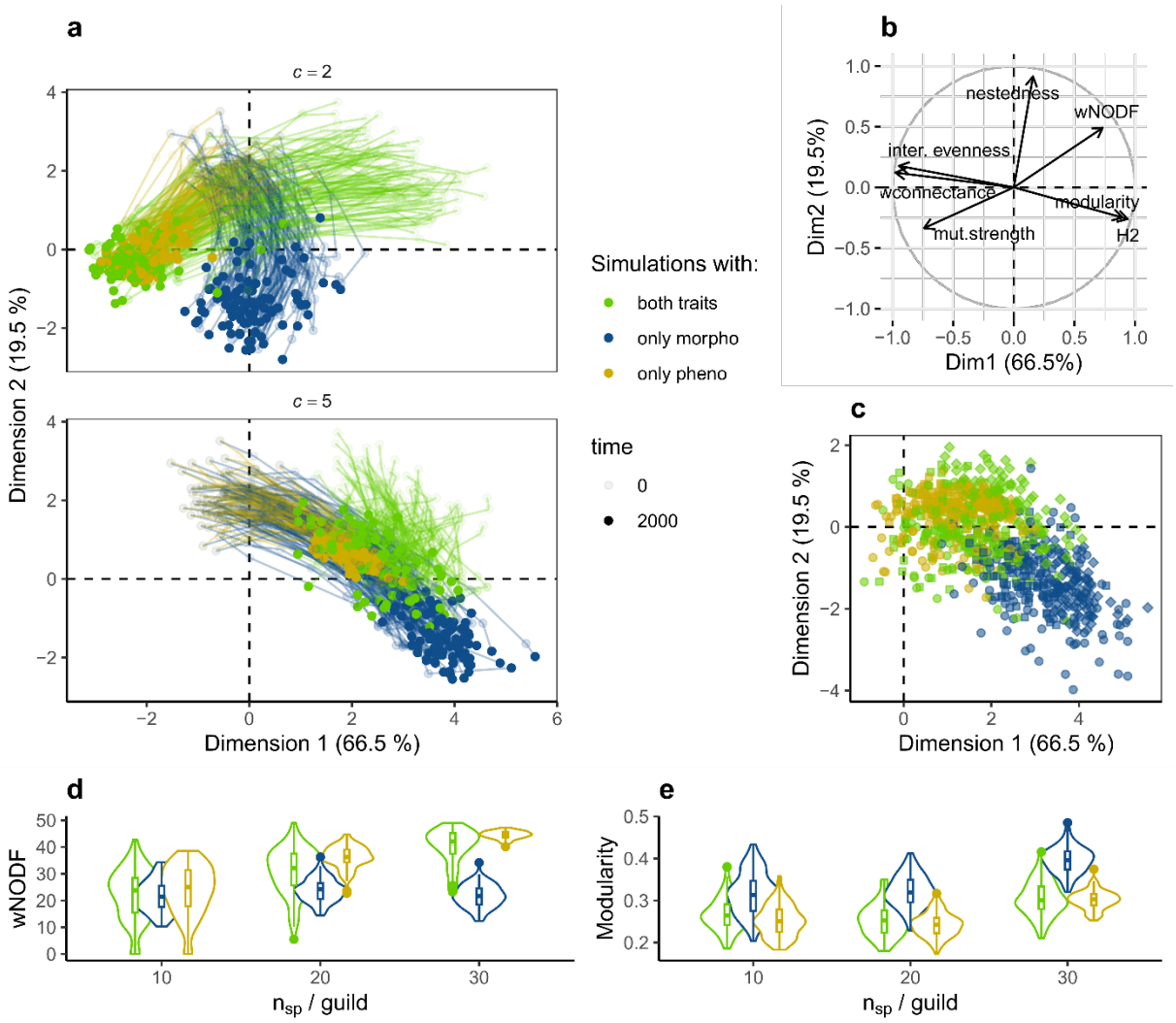

Fig. 1: phenological and morphological coevolution led to divergent evolutionary trajectories of communities. *(a) Location of each network at different time steps, in a multidimensional space of network structure, for different importance of competition (c = 2 & c = 5). The multidimensional space of network structure was created using the Principal Component Analysis (PCA) illustrated in (b). In (a) only the simulations with 30 species per guild are*

represented for readability. (b) PCA loading plot, where wNODF is a weighted measure of nestedness and H2 a measure of specialisation, and mut. strength a measure of connectance (cf. methods). (c) Final location of each community in the multidimensional space of network structure, when c = 5. Circles represent simulations with 10 species per guild, squares 20 species per guild and diamonds 30 species per guild. Cf. Figure S1 for final location of each community in the multidimensional space of network structure when c = 2. (d) and (e) represent the nestedness (measured as wNODF) and the modularity of the final networks, as a function of the number of species per guild and kind of trait, when c =5.

When coevolutionary dynamics unfolded, traits modifications quickly reorganize species interactions, affecting the community structure (Fig. 1). The structure of the emergent interaction networks is strongly dependent on the importance of the competition in the model, highlighting the role of competition in driving the coevolutionary trajectory (Fig. 1a). When competition played a minor role (c = 2) coevolutionary dynamics tended to maximize trait matching across a maximum of species, increasing the connectance of the mutualistic networks (Fig. 1a-b). In contrast when competition played an important role (c = 5), coevolutionary dynamics tended to produce more specialized interaction networks, with lower connectance (Fig. 1a-c).

However, regardless the effect of competition, our simulations highlighted significant differences across various aspects of network structure, between the scenarios including phenological traits (mixed or phenological coevolution) and the scenario with morphological traits only (Fig. 1). Mixed and phenological coevolution tended to produce mutualistic networks with a very similar structure, more nested and less modular than mutualistic networks produced by morphological coevolution (Fig. 1). These divergences in network structures can be understood by examining the distribution of species traits. Phenological and mixed coevolution tended to produce a few generalist species, which are needed to produce nested interaction networks, while morphological coevolution produced only specialist species (Fig. S2).

To understand how coevolution balance mutualism and competition, we then focus on simulations in which competition was important (c = 5), as it appears to be the case in many mutualistic systems (2, 24, 25). Under this case, mixed and phenological coevolution produced interaction networks with less mutualistic interactions but also less competition than morphological coevolution, leading to a positive mutualism-competition balance (Fig. 2c-e). In contrast, morphological coevolution led to a negative mutualism-competition balance with a ratio of mutualism over competition below one (Fig. 2c-e). Phenological and mixed coevolution produced more favorable mutualism-competition balance because they reorganized phenologies in a way that potential competitors did not overlap in time. This reorganization creates “V+” motifs that promote facilitation (Fig. 1e), patterns that cannot be produced by morphological coevolution.

These first results suggest that phenological coevolution is more likely to decrease the likelihood of competitive exclusion than morphological coevolution. Importantly, when both traits coevolved, the coevolutionary dynamics were mostly driven by phenological traits, suggesting that coevolution of species phenologies is key in determining emergent properties at community level.

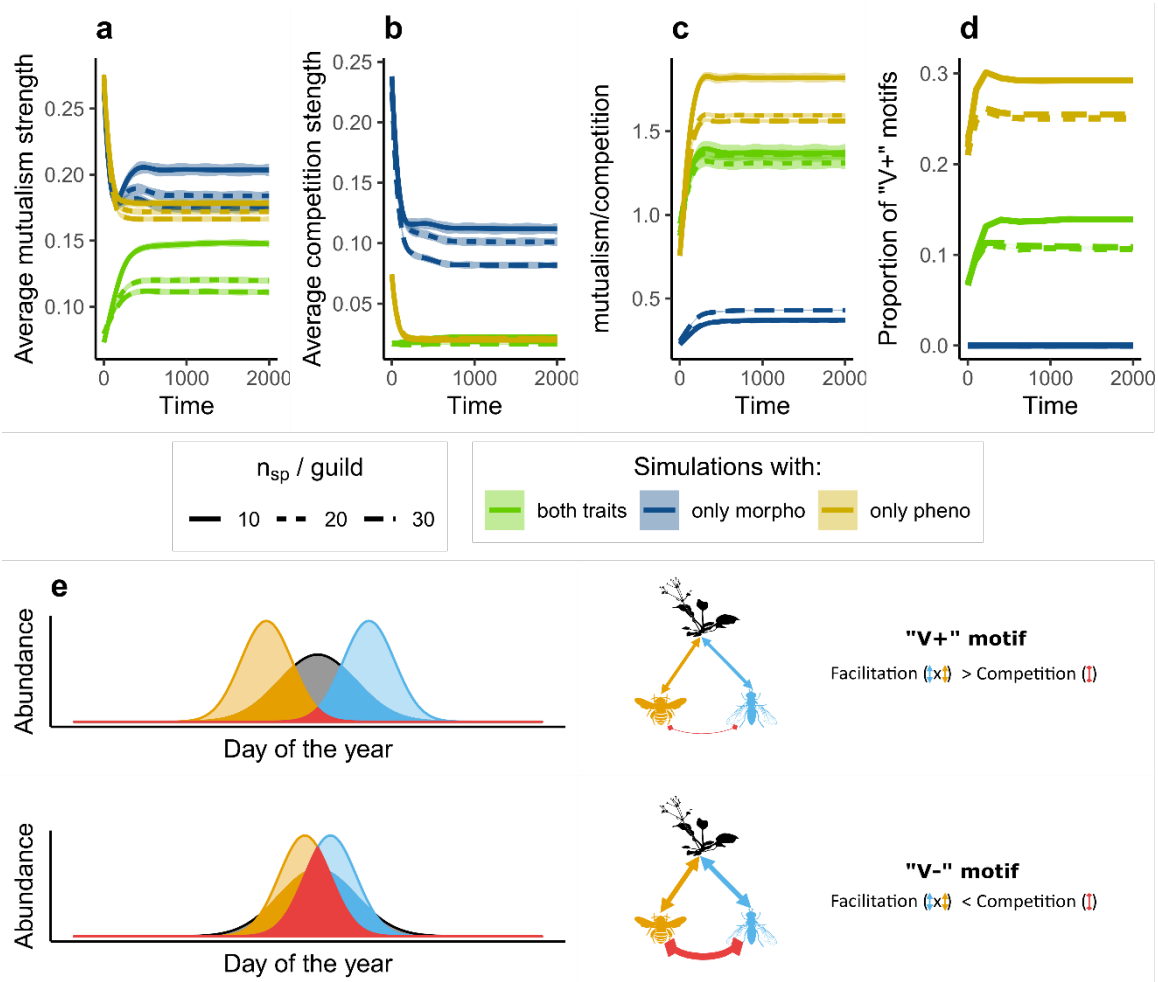

Fig. 2: motifs promoting facilitation emerge from phenological coevolution. *(a) average mutualistic strength, (b) average competition strength, (c) mutualism/competition balance (cf. methods) and (d) proportion of "V+" motifs, as a function of time, diversity and simulation scenarios. In (a)-(d) the lines and ribbon show the estimated values and their 95% confidence interval, respectively, obtained by a locally estimated scatterplot smoothing (LOESS) of the values across time. V+ motifs did not exist when performing coevolution with morphological trait only (cf. Methods). (f) Schematical examples of "V" motifs: on the top a "V" motif promoting facilitation ("V+"), and on the bottom a V motif promoting competition ("V-"). In the top, pollinators interact with the same plant but overlap little in time, and hence they almost do not compete but facilitate each other. The facilitation between pollinators is the positive indirect effect mediated by the plant (the product of the mutualistic interactions). In the bottom pollinators largely overlap in time, a structure which tend to promote competition over facilitation, which can lead to competitive exclusion.*

These divergence in network structure due to trait coevolution translated in differences in the structural stability of the communities (ω, Fig. 3). The initial structural stability was higher for communities structured by phenology (Fig. 3), because decoupling interactions in time, even randomly, decreases competition strength (Fig. 2b-c). However, what most interested us was seeing how coevolution shaped it, *i.e.* the trajectory over time of this structural stability. In a context of moderate or high interspecific competition, phenological and mixed evolution strongly increased structural stability, while morphological evolution did not have a clear effect (Fig. 3). This trajectory depended on the strength of the interspecific competition relative to the intraspecific competition (ρ) and on the importance of the competition in the model (*c*). However, phenological and mixed coevolution always led to higher structural stability than

morphological coevolution, excepting when both ρ and *c* were low, in which case all coevolution scenarios exhibited relatively similar structural stability (Fig. S3 & S4).

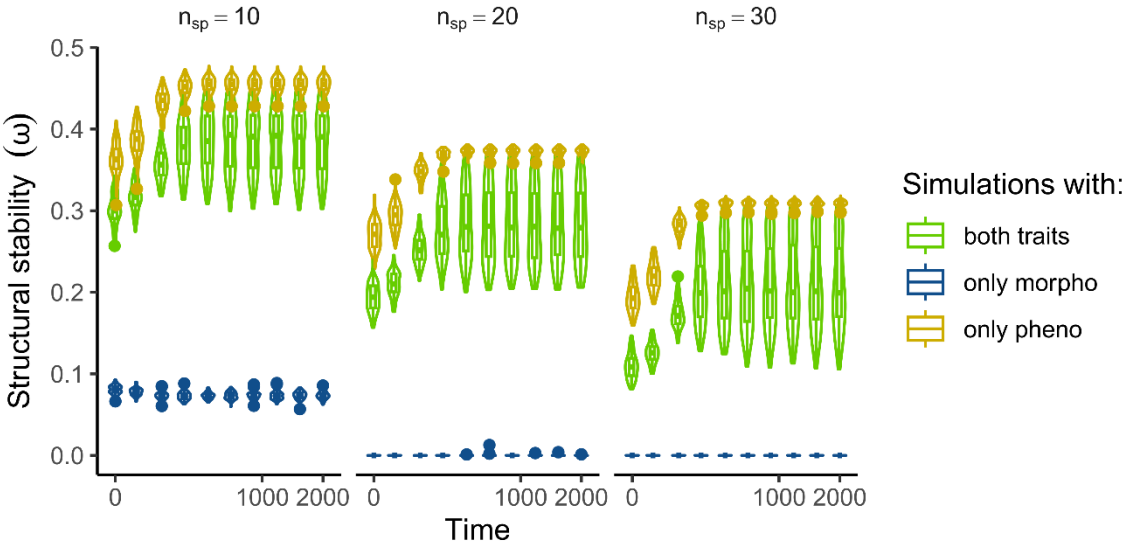

Fig. 3: phenological coevolution increased structural stability and dampened the diversity-stability trade-off. *Changes in structural stability (average persistent probability) over time, for the three coevolution scenarios and number of species per guild, when interspecific competition was relatively strong (ρ = 0.4). Simulation performed with an overall competition strength c = 5, see Fig. S4 for simulations with c = 2. The x-axis is square-root transformed.*

Importantly, in a context of realistic moderate to high interspecific competition, phenological and mixed coevolution also dampened the diversity-stability trade-off (Fig. 4). At initial conditions, the number of species per guild negatively affected the structural stability (Fig. 4a), which is a known relationship (26). However, in networks coevolved based on a phenological trait this relationship was attenuated (Fig. 4b). In contrast, the diversity stability trade-off was still strong in coevolved networks when considering a morphological trait (Fig. 4a & S5). This result suggests that coevolutionary dynamics can dampen the diversity-stability trade-off, when considering phenological coevolution but not when considering morphological coevolution.

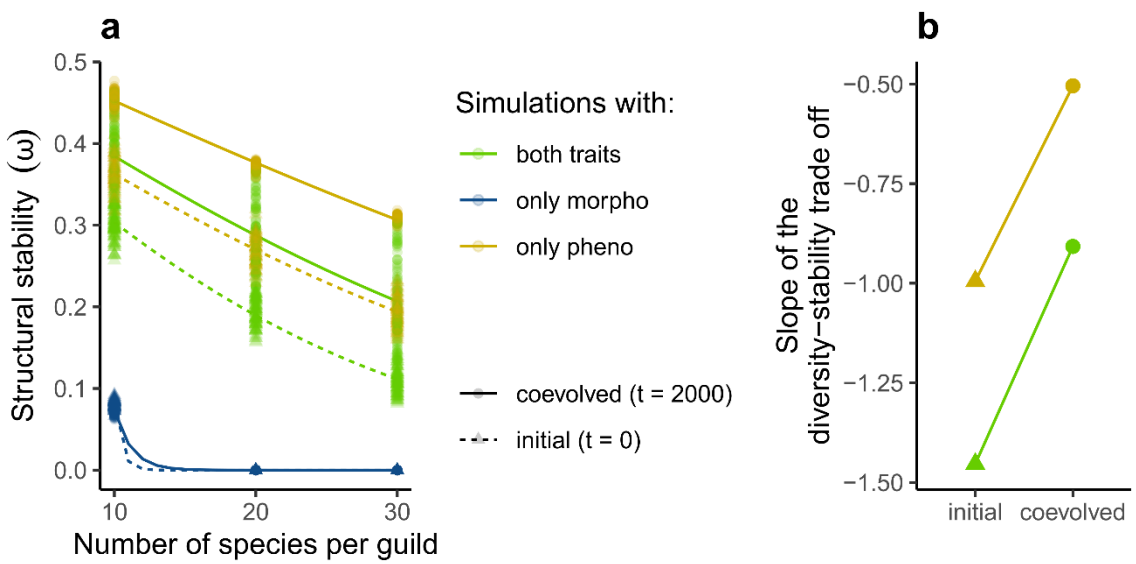

Fig. 5: Coevolution of phenologies dampened the diversity-stability trade-off. *(a) structural stability as a function of the number of species per guild (i.e. diversity), for interspecific competition strength ρ=0.4. Lines show the predictions of a Generalized Linear Model (GLM, cf. Methods). (b) Slopes of the diversity-stability relationships extracted from the GLM. We did not represent the slopes for the morphological coevolution to preserve readability, but in that case no change between initial and coevolved networks was observed (Fig. S5). In (b) error bars (±CI95%) are too small to be visible.*

Finally, to assess the stabilizing role of phenology on real-world communities, we analyzed the phenological organization of 17 empirical plant-pollinator networks (cf. Table S1). We found evidence for a high proportion of the "V+" motifs (Fig. 5a), described in Fig. 2d-e, which suggests that coevolution of species phenologies have shaped the seasonal structure of plant-pollinator interactions. Performing coevolutionary simulations with networks having the same number of species per guild as the empirical ones (*cf.* Methods), we show that the proportion of motifs promoting facilitation were relatively consistent with what was predicted by mixed coevolution and higher than what would be found in random initial networks (Fig. 5a).

We assessed the structural stability of empirical communities by either considering that all interactions occurred simultaneously (*i.e.* aggregated networks) or considering the observed seasonal structure in interactions (*cf.* Methods). As predicted by the simulations, considering the seasonal structure in interactions led to an increase in the structural stability of the empirical communities (Fig. 5b-c). This shows that the stabilizing role of the coevolved seasonal structures that we found *in silico* is likely to be important in stabilizing natural mutualistic communities. The positive effect of the seasonal structure on the structural stability increased with species diversity, which means that the seasonal structure was dampening the diversity-stability trade-off (Fig. 5b). This positive effect also increased with the strength of the interspecific competition (*ρ*, Fig. 5c), confirming that seasonal structures might be of particular importance in diverse communities and when competition for mutualistic partners is strong.

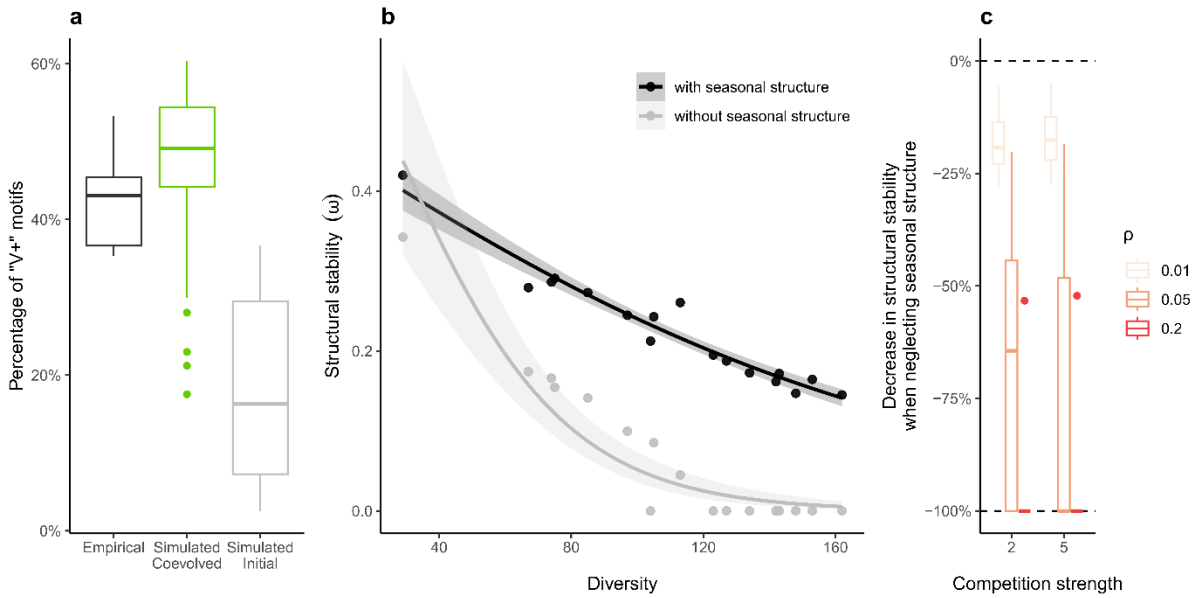

Fig. 5: Seasonal structure in interactions stabilize natural communities. *(a) Distribution of the percentage of "V+" motifs, relative to the total number of V motifs, in the 17 empirical networks, and in simulated networks with similar dimensions (cf. methods), before (i.e. random, grey) and after mixed coevolution (green). (b) Structural stability, average probability of persistence, as a function of community diversity (number of pollinator and plant species), when accounting for seasonal structure*

in competitive interactions or when neglecting this seasonal structure. For a given overall competition and interspecific competition strengths (c = 5 & ρ = 0.05). The lines and ribbon show the estimated values and their 95% confidence interval, respectively, obtained by generalized linear model with a quasi-binomial error structure. (c) The decrease in percentage of the structural stability observed when neglecting seasonal structure, relative to the measure when considering it, as a function of the overall competition strength (c parameter, cf. Methods) and of the interspecific competition strength (ρ, cf. Methods). n = 17 for each boxplot. Dots represent outliers.

Discussion

Our results show that explicitly modelling the linkage rules defining species interactions is important to understand the community level outcomes of coevolutionary dynamics. Using an integrative metric of ecological stability, we show that the structural stability of mutualistic communities was enhanced by phenological coevolution but was diminished by morphological coevolution. Our results highlight that a largely neglected ecological mechanism, the temporal organization of species interactions that emerges when phenological traits are considered, is key to understand coevolutionary dynamics and the stability of diverse mutualistic communities.

Phenological traits can decouple interactions in time, rendering an asymmetric partition between the mutualistic interactions and the competition for mutualistic partners (21, 27), in contrast to morphological traits. Surprisingly, this key mechanism for species coexistence has only recently been integrated to ecological models, but is now well recognized (10, 21, 28–31). However, the emergence of seasonal structures fostering stability from coevolutionary dynamics remained uncertain. Here we show that these community level patterns can emerge naturally from species fitness driven coevolution. In contrast, when considering only morphological traits, the coevolutionary dynamics drive the community towards modular and specialized networks with low stability. Our results thus suggest that coevolution of species phenology might be one of the main structuring factors of mutualistic networks, explaining how they can be diverse and stable together.

Using a set of 17 empirical networks, we found a high proportion of phenological motifs suggesting that interaction networks have been shaped by coevolution of species phenologies. These phenological motifs promoting facilitation were in a higher proportion than what would be found if phenologies would be distributed randomly, suggesting that phenological coevolution drives the emergence of stabilizing structure in these systems, consistently with our theoretical predictions. In these 17 plant-pollinator networks, neglecting the seasonal structure in interactions could lead to underestimating the structural stability of the empirical communities from ~10% to 100% depending on the community diversity and interspecific competition strength.

Importantly, our model did not include any abiotic constrain on phenologies other than physiological bounds. Thus, in our simulations, the emergence of seasonal structure was only driven by species interactions. This suggests that the mechanism we describe could be universal: seasonal structures in interactions are expected to be present in every mutualistic system where interspecific competition for mutualistic partners is high enough, regardless the abiotic seasonality. Since, interspecific competition for mutualistic partners has been reported to be strong in many different mutualistic systems, such as pollination (25), seed-dispersal (24, 32), mycorrhizae (33) and cleaner-client fishes (34) , we expect that these systems would exhibit

stabilizing seasonal structures. Our results could explain why even tropical mutualistic systems with relatively constant abiotic conditions, such as plant-hummingbird interactions, exhibit a strong seasonal structure (20), that increases community stability relative to hypothetic cases without or with random seasonal structure (30).

Our findings regarding how phenological coevolution increased community stability can be generalized to other kinds of traits, if they allow to decouple interactions with a common partner in time or space. For example, those can be traits associated with thinner temporal dynamics, such as daytime activity and flower opening (e.g. diurnal *vs*. night) or morphological traits with inter- or intra-individual variation, such as flower heights. These kinds of traits can also create "V+" motifs, maintaining mutualistic interaction with two different partners while removing direct competition between them. For instance, differences in flower heights in a tree could allow two pollinator species that fly at different heights to avoid competition while still interacting with the same tree population, if individuals have different heights, or even with the same individual tree, if it has flowers at different heights. This vertical stratification exists for example in plant-hummingbird interactions (35). Thus what we call here phenological and morphological trait could be also generalized as traits with and without inter-individual variation, respectively, which is consistent with recent results highlighting intraspecific variability as a key mechanism promoting the stability of plant-pollinator communities (36).

By showing that complex and collective structures fostering stability can emerge from species' fitness driven evolution, we effectively link coevolutionary mechanisms and community ecology. Most importantly, the emergence of these stabilizing structures depends on which kind of traits coevolve: while coevolution of morphological traits does not increase community stability, coevolution of phenologies tends to do so and dampen the diversity-stability trade-off. Overall, our results suggest that coevolutionary dynamics enhance the positive effect of seasonal structures on community stability (10, 21, 28–30), which is probably a key mechanism to understand how natural communities can be both diverse and stable.

Methods

We developed a coevolution model in lines with previous ones (14, 15, 37), which is intermediate between a coevolutionary model and community assembly model. In this model all species were assumed to have the same abundance, which was fix over time, while trait values are changing because of natural selection driven by mutualistic and competitive interactions. Our model simulated the reorganization of an interaction network of fixed dimensions (fixed set of species) due to coevolution. We could then calculate structural properties of that interaction network and the probability for that species assemblage to coexist (feasibility).

For simplicity we took the example of a plant-pollinator community, but the model could apply to any mutualistic community.

Species trait

Each species was characterized by two gaussian traits: a morphological trait and a phenological trait, with a mean μ_M and μ_P and a standard deviation σ_M and σ_P, respectively. Both traits evolved independently, *i.e.* we assumed no genetic covariance among them. To make comparisons possible between traits, both were treated exactly in the same way, on a scale that goes from 0 to 365. For phenology it obviously recalls the day of the years, while for morphology it can be any abstract scale.

To mimic physiological limits, we bounded the mean trait values between 80 and 285, and the standard deviation values from 1 to 50. To bound trait values without using a sharp truncation that would create weird behaviors at the bounds, we used a process inspired by generalized linear models, in which the trait evolves on an unbounded latent distribution linked to the effective bounded values through a link function. As a link function we used a modified logit function (*cf.* Supplementary Methods I). In the following part, μ and σ, denote the values on the bounded scale (real mean and standard deviation), while $\ddot{\mu}$ and $\ddot{\sigma}$ denote the value on the latent unbounded scale. For example, $\ddot{\mu}$ varied from $-\infty$ to $+\infty$, but μ was bounded between 80 and 285.

Species interactions

The overlap between their morphological (φ_{ij}) and phenological traits (τ_{ij}) determine the interaction strength (γ_{ij}) between a pollinator *j* and a plant *i*:

$$\gamma_{ij} = \varphi_{ij}\tau_{ij} \tag{1}$$

To calculate the overlap between traits, we used the area below the minimum of the two gaussian traits involved (Fig. 2e):

$$\tau_{ij} = \int_0^{365} min\left(\frac{1}{\sigma_{P_i}\sqrt{2\pi}} e^{\frac{-1}{2}\left(\frac{x-\mu_{P_i}}{\sigma_{P_i}}\right)}, \frac{1}{\sigma_j\sqrt{2\pi}} e^{\frac{-1}{2}\left(\frac{x-\mu_{P_j}}{\sigma_{P_j}}\right)}\right) dx \tag{2}$$

φ_{ij} was calculated according to an equation similar to equation (2).

This means that the mutualistic interaction strengths are bounded between zero and one ($0 \leq \gamma_{ij} \leq 1$), because φ_{ij} and τ_{ij} are bounded between zero and one.

The competition between plant i and k for pollinator j was defined as the geometric mean of their mutualistic interaction strengths with pollinator j (γ_{ij} and γ_{kj}), multiplied by their temporal co-occurrence (τ_{ik}). To calculate the overall competition coefficient (α_{ik}), we average those competition across all pollinators:

$$\alpha_{ik} = \tau_{ik} \frac{1}{n_A} \sum_{j=1}^{n_A} \sqrt{\gamma_{ij}\gamma_{kj}} \tag{3}$$

where n_A was the number of pollinator species. We set the intraspecific competition to one, $\alpha_{i,k=i} = 1$, to ensure diagonal dominance of our system. The competition coefficient among pollinator species was calculated with an equation similar to equation (2). These competition coefficients represent competition for mutualistic partners only, as here we ignored competition for abiotic resources or space, because we wanted to focus on the role of mutualistic interactions in driving coevolution.

Species fitness and trait evolution

The plant-pollinator population dynamics can be described by a generalized Lotka-Volterra model, as often done (6, 7). In this model, the variation in the population size of plant i, would be:

$$\frac{dN_i}{dt} = N_i \left(r_i - c \sum_{k=1}^{n_P} \alpha_{ik} N_k + \sum_{j=1}^{n_A} \gamma_{ij} N_j \right) \tag{4}$$

where r_i was the basal per-capita growth rate of species i, and c was the overall strength of the competition, relative to mutualism. The variation in population size of pollinators was described by a similar equation.

We did not solve that Lotka-Volterra model, because we fixed the population sizes to one ($N_i = 1, \forall i$), but we used the Lotka-Volterra model to define the fitness of species i (W_i), which was the total population growth rate. Since we were interested in the fitness components that depended on trait values only, the growth rate of the population could be summarized as the balance between competition and mutualism:

$$W_i = -c \sum_{k=1}^{n_P} \alpha_{ik} + \sum_{j=1}^{n_A} \gamma_{ij} \tag{5}$$

At each time steps we introduced independent mutations on trait parameters (μ_M, μ_P, σ_M and σ_P). For each parameter we introduced deterministic positive (e.g. $\mu_M + \varepsilon$) and negative mutations (e.g. $\mu_M - \varepsilon$), with a mutation size ε. We calculated the fitness associated with the three trait values, unmuted (resident), positive and negative mutation. Among these three values, we kept the trait parameter value associated with the highest fitness for the next time step.

Simulations with only one trait

We first performed simulation with only one trait, either morphological or phenological, to compare their coevolutionary dynamics in isolation. To neglect phenology when simulating

with a morphological trait we set $\tau = 1$ for all pairs of species, meaning that all interactions occur simultaneously. In contrast, to ignore morphology when simulating with a phenological trait we set $\varphi = 1$, meaning that all species have a perfect morphological match.

We performed simulations over 2000 time steps. In our time-discrete model, traits values never reach an equilibrium because all species traits change simultaneously, but the trait evolution was fast in the first 200 steps, before slowing down and reaching stationary states (Fig. S6). We performed simulations over a set of 100 random initial combinations of traits values. We drew initial trait values on the modified logit scale (*cf.* Supplementary Methods I) from a uniform distribution for the mean and the standard deviation: $\ddot{\mu}_{i,t=0} \sim U(-2.5,2.5)$ and $\ddot{\sigma}_{i,t=0} \sim U(-2.5,2.5)$. We generated 100 initial conditions for 3 different values of initial diversity: 10, 20 and 30 species per guild. For each initial condition, the simulation was run twice, considering a morphological trait or a phenological trait.

Simulations with two traits

To assess the interaction between the coevolutionary dynamics of the morphological and phenological trait, we performed simulations with both traits coevolving. We used the same 100 initial conditions for 3 different values of initial diversity as before, for phenology and morphological traits.

Parametrization of the simulations

Our simulations required very few parameterizations, because most of the coefficients were determined by the evolving trait values. However, we needed to choose a value for competition strength, the parameter c in equations (4) and (6). Since our competition coefficients are always smaller than the mutualistic interaction strength (*cf.* equation (2)), we needed $c>1$ to avoid mutualistic orgies, a common behaviour in linear models of mutualistic communities (38). A mutualistic orgy would lead to get all the species quickly converging to the same trait value and would thus not be realistic. We performed simulations for a relatively low importance of the competition in the model ($c = 2$) and a high importance ($c = 5$).

The mutation size ε was fixed to 0.01, which allows a smooth evolution (without big jump due to high mutation size) but fast enough to allow simulation to reach a stationary state (Fig. S7).

Network structure

To assess how coevolutionary dynamics affect the structure of the interaction network, we measured indices describing the mutualistic interaction network. Since our interaction networks were fully connected but sometimes with links that were extremely weak, we rounded the interaction strengths (γ_{ij}) to the third digit to set to zero all $\gamma_{ij} \leq 0.0005$. We measured the weighted connectance, nestedness, modularity, specialization and interaction evenness of the mutualistic networks. As different indices gave different information, we measured nestedness using two different indices, the index proposed by Galeano *et al.* (39) and the wNODF (40). All these indices were computed with the *bipartite* R package (41). The weighted connectance metric implemented in the *bipartite* R package is not sensitive to shifts in scale but only to the distribution of interactions. To track how coevolutionary dynamics was affecting the strength of mutualism we also calculated the average mutualism strength, which is the average of all γ_{ij} and be view as a second metric of connectance.

Since evolution slowed down with time (Fig. S5), we measured these metrics at 10 time steps, that were evenly distributed on a square-rooted time scale (t = 0, 20, 100, 220, 400, 620, 890, 1210, 1580, 2000). To track network structure over time, we performed a Principal Component Analysis (PCA) with the seven metrics described above, across all simulations and time steps. We used the two first dimensions of this PCA which explained 86% of the total variance, to characterize the evolutionary trajectories of the simulated communities.

Mutualism-competition balance and motifs promoting facilitation

To assess how coevolutionary dynamics balance mutualism and competition at the community level, we also calculated the average competition strength, which the average of all α_{ij}, and the balance between mutualism and competition as $\frac{\gamma_{ij}}{c\alpha_{ij}}$.

To test if co-evolutionary dynamics can lead to phenological motifs that promote facilitation over competition, we calculate the number of motifs with a "V" shape promoting facilitation, or "V+" motifs (Fig. 2e). This kind of motifs can be present only in the phenological scenario. In contrast, when considering morphological traits, all interactions happen simultaneously ($\tau = 1$) and thus competition between two species from the same guild does not depend on their trait overlap but only depends on their overlap in mutualistic interactions.

Since our in-silico mutualistic networks were weighted and without real zeros, we had to put a threshold above which we consider mutualistic interactions were strong enough to constitute "V" shape motifs. We used only the links for which $\gamma > 0.01$ and we extracted all corresponding "V" motifs. We calculated the number of "V+" motifs as those where the two species from the same guild overlapped less in their trait value than the product of their overlap with their mutualistic partner. For example, a "V" motif in which a plant *i* interact with pollinators *j* and *k* would be "V+" motif if $\gamma_{ij}\gamma_{ik} > \tau_{jk}$, and "V-" motif otherwise (see Fig. 1). As connectance was changing among simulations because of different initial conditions, and within simulations, because of coevolutionary dynamics, we estimated the proportion of "V+" motifs, over the total number of motifs with a "V" shape. This allowed to get comparable measures over time and across simulations.

Structural stability

To understand how evolutionary dynamics affect the ecological stability of our system, we measured the community structural stability. Structural stability is a measure of ecological stability that aims to quantify the range of environmental conditions, modelled through the per capita basal growth rates (*r*), in which all species can coexist in a stable way (7, 8, 42). The range of environmental conditions, or growth rates, in which all species can coexist is call the feasibility domain, and the structural stability is quantified as the size of the feasibility domain scaled by the number of species in the community, which gives an average measure of species persistence.

To calculate the structural stability of our communities, we used the generalized Lotka-Volterra model used to derivate fitness gradients, presented in equation (4). Since the structural stability metric already accounts for competition for mutualistic partners via matrix multiplication and inversion (43), for competition coefficients we used a mean field structured by phenological overlap: $\alpha_{ik} = \tau_{ik}\rho$, where ρ is the interspecific competition strength. As

before, we set $\alpha_{i,k=i} = 1$, and we calculated structural stability for different values of the interspecific competition $\rho \epsilon$ [0.01,0.05,0.2,0.4,0.6].

The vector of species abundances at equilibrium (N^*) was given by $N^* = A^{-1}r$, where r was the vector of species growth rates and A was the adjacency matrix describing within guild interaction (competition) as well as between guilds interactions (mutualism) among all pairs of species. This matrix was composed by four blocks:

$$A = \begin{bmatrix} -c\alpha_{(P)} & \gamma \\ \gamma^T & -c\alpha_{(A)} \end{bmatrix} \quad (6)$$

where $\alpha_{(P)}$ was the competition matrix among plants, dimensions of $n_P \times n_P$, and $\alpha_{(A)}$ was the competition matrix among pollinators ($n_A \times n_A$). γ was the mutualistic interaction matrix ($n_P \times n_A$), and γ^T its transposed.

The feasibility domain is the range of vectors r that give N^* with positive species' abundances only. The size of the feasibility domain ($\Omega(A)$), was calculated as follow:

$$\Omega(A) = \frac{vol\left(D_f(A) \cap B^S\right)}{vol(B^S)} \quad (7)$$

where $D_f(A)$ was the feasibility domain of A and B^S was the closed unit ball in dimension $S = n_P + n_A$.

To quantify structural stability, we normalized the size of the feasibility domain by the number of species in the community: $\omega(A) = \Omega(A)^{1/S}$. The normalized feasibility, $\omega(A)$, is bounded between 0 and 1 and corresponds to the average species persistence probability in the community, represented by the interaction matrix A. The closer the feasibility is to one, the more likely is that all species will coexist in a stable way. To compute this normalized feasibility, we used the *Omega* R function provided by Song *et al.* (42).

Diversity-Stability trade off

To study how coevolution affected the relationships between the structural stability and the diversity, we explained the structural stability by the diversity using a Generalized Linear Model (GLM) with a quasibinomial error structure and a logit link function. To model one diversity-stability trade off per coevolution scenario, for initial and coevolved networks, we included a triple interaction between the diversity (number of species per guild), the kind of coevolution scenario and the kind of network (initial *versus* coevolved). The GLM was described by the following equation:

$$logit\left(\omega(A)_{tij}\right) \sim \beta_{0_{ti}} \times diversity_j \quad (8)$$

where $\omega(A)_{tij}$ was the structural stability at time *t*, initial (*t* = 0) or coevolved networks (*t* = 2000), for coevolution scenario *i* (phenological, morphological or mixed coevolution) for diversity *j*. $\beta_{0_{ti}}$ was the slope of the diversity-stability relationships, on a logit scale, for each time *t* and coevolution scenario *i*.

Analyses of empirical plant-pollinator interaction networks

We used a set of 17 time-structured plant-pollinator interaction networks, sampled in the area of the Doñana National park, near Sevilla, in Spain, with the protocol described in *ref.* (44). These networks have been sampled at bi-weekly intervals during the peak season (February to May), for one to 8 years (Table S1). Interactions have been recorded at each sampling occasion along a 100m transect during 30 effective minutes, and flower abundances per species have also been recorded along that transect in a standardized way (44). To calculate the structural stability of the empirical networks, we ideally want to get mutualistic interaction strengths that do not depend on sampling effort, neither on species abundances. To correct interaction strength by sampling effort, we calculated the average number of detected interaction per sample round: $\overline{I_{ij}} = \frac{1}{N}\sum_{s=1}^{N} I_{ijs}$, where N is the number of sampling events, and I_{ijs} the number of interactions detected between plant i and pollinator j during sampling event s. To account for species abundances, we divided the average number of interactions by the geometric mean of the marginal sums of species involved in the focal interaction:

$$\gamma_{ij} = \frac{\overline{I_{ij}}}{\sqrt{\sum_{i=1}^{n_P} \overline{I_{ij}} \times \sum_{j=1}^{n_A} \overline{I_{ij}}}} \tag{8}$$

If evolution of phenologies drove, at least partially, the seasonal organization of the interactions, we expect to find a non-negligible proportion of "V+" motifs (Fig. 1a), in line with what we found in coevolved seasonal structures. To do so, we estimated species phenologies. Since sites were all in the same geographical region (maximal pairwise distance was 53km), we assumed that phenologies were the same in all sites and thus we used all the data available to infer phenological parameters, which allows to get more precise phenological estimates per species. We also assumed gaussian phenologies for all species, meaning that we had to estimate only two parameters, the mean and the standard deviation (cf. Supplementary Methods II).

Once we have estimated the species phenologies, we count the number of "V+" motifs, in which the (geometric) average overlap between mutualistic partners was higher than the overlap between the two competitors. To get a measure comparable with our simulations and among networks, as before, we estimated the proportion of "V+" motifs over the total number of "V" shape motifs.

Finally, to see how considering the seasonal structure in interactions affected the structural stability of these communities, we estimated the feasibility (ω) with and without considering the seasonal structure in the interactions. This seasonal structure did not affect the mutualistic interactions (γ_{ij}), as they already depended on phenologies, but only the mean field of competition, which was calculated as in the simulations with $\alpha_{ik} = \tau_{ik}\rho$, and $\alpha_{i,k=i} = 1$. As in simulations, to neglect the seasonal structure in interactions we set $\tau_{ik} = 1$, and to include the seasonal structure in interactions we calculated τ_{ik} according to equation (2) while using empirical phenologies. We used the generalized linear Lotka-Volterra from equation (4) to calculate the structural stability of the community, with and without seasonal structure in interactions in the same way as described previously, for different values of c and different values of ρ (Fig. 5).

Simulations with empirical networks dimensions

Finally, to compare the structure of the empirical networks with the structure obtained by phenological and morphological coevolution, we performed a new set of simulation using the number of plant and pollinator species of the empirical networks. We performed these simulations with $c = 5$, for a set of 10 different random initial conditions (traits values) for each of the 17 empirical networks.

Acknowledgements

We thank Nerea Montes for the help while collecting data. We also thank the taxonomists L. O. Aguado and T. Wood for their help with some bee identifications. FD was funded by *postdoc Mobility* grant from the SNF (project number: P500PB_217801), and VDG by a Marie Skłodowska-Curie grant (N°101064340) from the European Union's Horizon 2021 research. Data collection was funded by a Marie-Curie Career Integration from the European Union's Horizon 2020, the BeeFUN project (PCIG 14-GA-2013-631653), granted to IB.

References

1. C. Darwin, On the Various Contrivances by which British and Foreign Orchids are fertilised by Insects, and on the good effects of intercrossing ... With illustrations (John Murray, 1862).

2. E. I. Jones, J. L. Bronstein, R. Ferrière, The fundamental role of competition in the ecology and evolution of mutualisms. Annals of the New York Academy of Sciences **1256**, 66–88 (2012).

3. N. Loeuille, Influence of evolution on the stability of ecological communities. Ecology Letters **13**, 1536–1545 (2010).

4. S. L. Nuismer, B. Week, M. A. Aizen, Coevolution Slows the Disassembly of Mutualistic Networks. The American Naturalist **192**, 490–502 (2018).

5. S. Suweis, F. Simini, J. R. Banavar, A. Maritan, Emergence of structural and dynamical properties of ecological mutualistic networks. Nature **500**, 449–452 (2013).

6. U. Bastolla, et al., The architecture of mutualistic networks minimizes competition and increases biodiversity. Nature **458**, 1018–1020 (2009).

7. R. P. Rohr, S. Saavedra, J. Bascompte, On the structural stability of mutualistic systems. Science **345** (2014).

8. S. Saavedra, R. P. Rohr, J. M. Olesen, J. Bascompte, Nested species interactions promote feasibility over stability during the assembly of a pollinator community. Ecology and Evolution **6**, 997–1007 (2016).

9. E. Thébault, C. Fontaine, Stability of Ecological Communities and the Architecture of Mutualistic and Trophic Networks. Science **329**, 853–856 (2010).

10. F. Encinas-Viso, T. A. Revilla, R. S. Etienne, Phenology drives mutualistic network structure and diversity: Effects on the dynamics of mutualistic networks. Ecology Letters **15**, 198–208 (2012).

11. C. Song, R. P. Rohr, S. Saavedra, Why are some plant–pollinator networks more nested than others? Journal of Animal Ecology **86**, 1417–1424 (2017).

12. I. Bartomeus, S. Saavedra, R. P. Rohr, O. Godoy, Experimental evidence of the importance of multitrophic structure for species persistence. PNAS **118** (2021).

13. L. P. Medeiros, G. Garcia, J. N. Thompson, P. R. Guimarães, The geographic mosaic of coevolution in mutualistic networks. Proc. Natl. Acad. Sci. U.S.A. **115**, 12017–12022 (2018).

14. P. R. Guimarães, M. M. Pires, P. Jordano, J. Bascompte, J. N. Thompson, Indirect effects drive coevolution in mutualistic networks. Nature **550**, 511–514 (2017).

15. C. S. de Andreazzi, J. Astegiano, P. R. Guimarães Jr., Coevolution by different functional mechanisms modulates the structure and dynamics of antagonistic and mutualistic networks. Oikos **129**, 224–237 (2020).

16. S. L. Nuismer, P. Jordano, J. Bascompte, Coevolution and the Architecture of Mutualistic Networks. Evolution **67**, 338–354 (2013).

17. A. Mougi, Stability of an adaptive hybrid community. Sci Rep **6**, 28181 (2016).

18. F. S. Valdovinos, P. M. de Espanés, J. D. Flores, R. Ramos-Jiliberto, Adaptive foraging allows the maintenance of biodiversity of pollination networks. Oikos **122**, 907–917 (2013).

19. P. J. CaraDonna, et al., Interaction rewiring and the rapid turnover of plant–pollinator networks. Ecology Letters **20**, 385–394 (2017).

20. J. Sonne, et al., Ecological mechanisms explaining interactions within plant–hummingbird networks: morphological matching increases towards lower latitudes. Proceedings of the Royal Society B: Biological Sciences **287**, 20192873 (2020).

21. F. Duchenne, C. Fontaine, E. Teulière, E. Thébault, Phenological traits foster persistence of mutualistic networks by promoting facilitation. Ecology Letters **24**, 2088–2099 (2021).

22. J. A. Elzinga, et al., Time after time: flowering phenology and biotic interactions. Trends in Ecology & Evolution **22**, 432–439 (2007).

23. N. de Manincor, et al., Does phenology explain plant–pollinator interactions at different latitudes? An assessment of its explanatory power in plant–hoverfly networks in French calcareous grasslands. Oikos **129**, 753–765 (2020).

24. R. J. Warren II, I. Giladi, M. A. Bradford, Competition as a mechanism structuring mutualisms. Journal of Ecology **102**, 486–495 (2014).

25. M. Henry, G. Rodet, Controlling the impact of the managed honeybee on wild bees in protected areas. Scientific Reports **8**, 9308 (2018).

26. M. Dougoud, L. Vinckenbosch, R. P. Rohr, L.-F. Bersier, C. Mazza, The feasibility of equilibria in large ecosystems: A primary but neglected concept in the complexity-stability debate. PLOS Computational Biology **14**, e1005988 (2018).

27. C. Payrató-Borràs, C. Gracia-Lázaro, L. Hernández, Y. Moreno, Beyond the aggregated paradigm: phenology and structure in mutualistic networks. J. Phys. Complex. **5**, 025013 (2024).

28. S. Saavedra, R. P. Rohr, M. A. Fortuna, N. Selva, J. Bascompte, Seasonal species interactions minimize the impact of species turnover on the likelihood of community persistence. Ecology **97**, 865–873 (2016).

29. V. H. W. Rudolf, The role of seasonal timing and phenological shifts for species coexistence. Ecology Letters **22**, 1324–1338 (2019).

30. F. Duchenne, R. O. Wüest, C. H. Graham, Seasonal structure of interactions enhances multidimensional stability of mutualistic networks. Proceedings of the Royal Society B: Biological Sciences **289**, 20220064 (2022).

31. R. Ramos–Jiliberto, P. M. de Espanés, M. Franco–Cisterna, T. Petanidou, D. P. Vázquez, Phenology determines the robustness of plant–pollinator networks. Scientific Reports **8**, 14873 (2018).

32. J. H. Ness, W. F. Morris, J. L. Bronstein, Integrating quality and quantity of mutualistic service to contrast ant species protecting Ferocactus wislizeni. Ecology **87**, 912–921 (2006).

33. A. E. Bennett, J. D. Bever, Trade-offs between arbuscular mycorrhizal fungal competitive ability and host growth promotion in Plantago lanceolata. Oecologia **160**, 807–816 (2009).

34. T. C. Adam, S. S. Horii, Patterns of resource-use and competition for mutualistic partners between two species of obligate cleaner fish. Coral Reefs **31**, 1149–1154 (2012).

35. S. Thiel, et al., Vertically stratified interactions of nectarivores and nectar-inhabiting bacteria in a liana flowering across forest strata*. American Journal of Botany **111**, e16303 (2024).

36. B. Arroyo-Correa, I. Bartomeus, P. Jordano, E. F. Cagua, D. B. Stouffer, Integrating intraspecific variation into population dynamics reveals how interacting species persist in mutualistic communities. [Preprint] (2024). Available at: https://www.biorxiv.org/content/10.1101/2024.09.12.612448v1 [Accessed 6 November 2024].

37. L. G. Cosmo, et al., Indirect effects shape species fitness in coevolved mutualistic networks. Nature **619**, 788–792 (2023).

38. I. Scheuring, "The orgy of mutualism" as an artefact: a stage structured model of plant-pollinator and seed-dispersal systems. Abstracta Botanica **16**, 65–70 (1992).

39. J. Galeano, J. M. Pastor, J. M. Iriondo, Weighted-Interaction Nestedness Estimator (WINE): A new estimator to calculate over frequency matrices. Environmental Modelling & Software **24**, 1342–1346 (2009).

40. M. Almeida-Neto, P. Guimarães, P. R. Guimarães Jr, R. D. Loyola, W. Ulrich, A consistent metric for nestedness analysis in ecological systems: reconciling concept and measurement. Oikos **117**, 1227–1239 (2008).

41. C. F. Dormann, B. Gruber, J. Fründ, Introducing the bipartite Package: Analysing Ecological Networks. R News **8**, 4 (2008).

42. C. Song, R. P. Rohr, S. Saavedra, A guideline to study the feasibility domain of multi-trophic and changing ecological communities. Journal of Theoretical Biology **450**, 30–36 (2018).

43. J. Bascompte, A. Ferrera, "A structural theory of mutualistic networks" in Theoretical Ecology, (Oxford University Press, 2020).

44. V. Domínguez-Garcia, F. P. Molina, O. Godoy, I. Bartomeus, Interaction network structure explains species' temporal persistence in empirical plant–pollinator communities. Nat Ecol Evol **8**, 423–429 (2024).